

TMS2006

135th Annual Meeting & Exhibition

TMS Technical Division Student Poster Contest

**Gallery “Showing” by Student Authors
March 13, 2006 / 5 to 6:30 p.m.**

Sponsors

Electronic, Magnetic & Photonic Materials Division

Extraction & Processing Division

Light Metals Division

Materials Processing & Manufacturing Division

Structural Materials Division



Welcome

Friends,

On behalf of TMS and our five technical divisions, welcome to the gallery showing of entries in the first TMS Technical Division Student Poster Contest. The competition is divided into both undergraduate and graduate categories within each division. This new event was created to engage our student members in a creative competition to effectively convey their research, and to increase interaction between students and professional members. This directory and the posters on display are arranged alphabetically by division and then by category.

Prizes are awarded as follows:

Electronic, Magnetic & Photonic Materials Division

Graduate Student - \$500

Undergraduate Student - \$500

Extraction & Processing Division

Graduate Student - \$500

Undergraduate Student - \$500

Light Metals Division

Graduate Student - \$500

Undergraduate Student - \$500

Materials Processing & Manufacturing Division

Graduate Student - \$500

Undergraduate Student - \$500

Structural Materials Division

Graduate Student - \$500

Undergraduate Student - \$500

Best of Show - \$2,500

Two posters will be selected from among the 11 winners, and those student authors will represent TMS at the Jr. EUROMAT conference this September in Lausanne, Switzerland!

Thank you, and good luck to all our student authors!



Alexander R. Scott
TMS Executive Director

Student Technical Division Poster Contest: EMPMD - Graduate Level

(1) Three-Dimensional (3D) Microstructure Visualization of Sn-Rich Pb-Free Solder Alloys: Rajen S. Sidhu¹; Martha A. Dudek¹; Nikhilesh Chawla¹; ¹Arizona State University

Graduate Student Division. The properties of Sn-rich solders are controlled by their microstructure, which consists of an intermetallic phase in a Sn-rich matrix. Thus, it is necessary to accurately characterize intermetallic size, distribution, morphology and orientation. Traditional methods of quantitative microstructure characterization involve the use of two-dimensional (2D) images. Such representations can severely oversimplify irregular microstructural features. A three-dimensional (3D) microstructure visualization technique utilizing serial sectioning was developed to reconstruct and visualize the 3D microstructure of two intermetallics in Sn-rich alloys: Ag₃Sn in Sn-3.5Ag, and LaSn₃ in a novel Sn-rich La-containing solder. The 3D virtual microstructure accurately represented the morphology, alignment and distribution of intermetallic particles. * Research sponsored by the National Science Foundation and Semiconductor Research Corporation.

(2) Correlation of Mechanical and Microstructural Properties with Magnetic Properties for FeCo/Ru Multilayers : Jinmei Dong¹; Mrugesh Desai¹; Subhadra Gupta¹; Venkateswara Inturi²; ¹University of Alabama; ²Seagate Technology

Soft, high moment thin films of FeCo with various seed layers have been studied intensively for potential applications as poles in write heads. We have sputter-deposited multilayers of Ru/FeCo, and measured stress, grain size, texture, magnetostriction, and other magnetic properties of the multilayers as a function of Ru seed layer thickness, FeCo thickness, number of laminations and deposition conditions. Under optimized deposition conditions, Ru films have compressive stress and FeCo films have tensile stress. It is therefore possible to tailor the individual thicknesses to minimize the overall stress of the laminated structure. Our calculated estimates of the total stress, based on stress coefficients derived from initial data, agree very well with the experimentally measured values. We will present results showing the correlation of mechanical and microstructural properties with magnetic properties.

(3) Dissolution of Copper from Substrate Surfaces into Lead-Free Solder Joints: Ajay Garg¹; Iver Anderson²; Joel Harringa²; Alfred Kracher²; Douglas Swenson¹; ¹Michigan Technological University; ²Ames Laboratory

Although localized Cu dissolution is often reported, this study is an effort to quantify the change in bulk joint matrix composition that results from common Pb-free soldering practice, i.e., joining of Cu substrates by Sn-Ag-Cu (SAC) solder during simulated surface mount conditions. Four different SAC solder alloys (in wt.%): Sn-3.0Ag-0.5Cu, Sn-3.7Ag-0.9Cu, Sn-3.9Ag-0.6Cu, and Sn-4.0Ag-0.5Cu, were investigated, with Sn-3.5Ag as a baseline. A protocol for quantitative analysis of this complex microstructural region was established by comparing electron microprobe measurements in spot and broad beam modes and as-polished and lightly etched specimens. The average Cu content of the joint was found to be significantly higher than that of each solder alloy. Thus, initial contact of molten solder with the substrate appears effective for dissolution of Cu, in spite of rapid formation of an intermetallic phase as a diffusion barrier at each solder/substrate interface.

(4) Functionalized Singlewall Carbon Nanotubes for Toxic Gas and Relative Humidity Detection: Harindra Vedala¹; Ved Prakash Verma²; Somenath Roy¹; WonBong Choi¹; ¹Florida International University

In this work surface modified carbon nanotubes are used for the carbon monoxide and relative humidity detection. Carbon monoxide, on inhalation results in formation of carboxyhemoglobin in human body leading to fatality at high concentrations. The sensor device was fabricated by selectively coating SWNTs with oxide thin films and polymer (Poly Vinyl Alcohol) by using e beam lithography and thin film deposition technique to enhance the sensitivity and selectivity of the sensor. The change in the electrical conductance of SWNTs was used as sensor response to CO at very low concentrations (below 100 ppm range). This sensor provides a dual purpose of sensing CO and relative humidity along with the elimination of the effect of the latter, a major interferent, on CO response. The effect of temperature and film thickness is examined. The sensing response mechanism is also discussed.

(5) Electromigration Induced High Reactive Diffusion Path in Sn-In/Cu Joints : Shih-Kang Albert Lin¹; Sinn-Wen Chen¹; ¹National Tsing Hua University

In-Sn alloys are promising lead-free solders in low temperature soldering application. Cu is common used as under bump metallurgy (UBM) in electronic packaging. Interfacial reaction occurs at the In-Sn/Cu joints of electronic products during electric current stressing. Not only Joule heating but also electromigration effect contributes to intermetallic compounds (IMCs) growth. The poster exhibits the results of electromigration effect upon interfacial reactions in Sn-In/Cu joints. Same intermetallic phase, η -Cu₆(Sn,In)₅, formed at interface with or without electrifying. By the compositional analyses, the same intermetallic phase formed at both electric directions. However, it is significant morphological difference at interface stressed by up-stream and down-stream of electric current. When electrons flew from In-Sn solder to Cu substrate, the reaction layer is flatter and similar to that without electrifying. On the other hand, when electrons flew in reversed direction, the IMCs grew along solder grain boundaries.

Student Technical Division Poster Contest: EMPMD - Undergraduate Level

(6) Study of Electrical Resistivity and Hardness of Cu-Nb Cold Roll Bonded Multi-Layered Materials: *Michael R. Henderson*¹; *Viola L. Acoff*¹; ¹University of Alabama

By utilizing cold roll bonding, copper and niobium foils were bonded together to form multi-layers. These Cu-Nb multi-layers, which ranged in thickness from 68 μm to 865 μm , exhibited interesting properties. The properties of the multi-layered structures are of interest because they are unique compared to the properties of the individual layers. The microhardness values and the resistance values were determined for each sample and were evaluated as a function of number of layers. The measured resistance decreased as the number of layers in the multi-layered structure increased. The measured values for resistance ranged from 52 μO for the highest number of layers to 372 μO for the smallest number of layers. These measured resistance values were compared to the calculated resistance values and the observed trend correlated with the calculated trend. The average microhardness was found to increase with increasing number of layers.

(7) Imaging Charge Carrier Transport in Single Intrinsic Semiconductor Nanowires: Carrier Mobility and Lifetime: *John P. Romankiewicz*²; *Yi Gu*¹; *Lincoln Lauhon*¹; ¹Northwestern University

By locally imaging the charge transport using the scanning photocurrent microscopy technique, we have directly measured the mobility-lifetime product for both electrons and holes in intrinsic semiconductor nanowires for the first time. The effective electron-hole separation by the electric field in ohmic devices contributes to the enhanced carrier lifetime, and this is confirmed by studying nanowire Schottky diodes, where the electric field distribution can be controlled by external bias. These studies represent the first and an important step towards the experimental test of the predicted superior carrier mobility in 1-D nanomaterials and the ultimate performance potential of semiconductor nanowire devices.

(8) A Review of Conducting Polymers: *Jacqueline L. Milhans*¹; ¹Carnegie Mellon University

Conducting and semi-conducting polymers have become of significant interest in the past decade. Some advantages to using electronic polymers include their ability to provide lightweight, thinner, and cheaper electronics. In this review, polyacetylenes, polythiophenes, and polypyrroles are explored, regarding synthesis, structure, conduction mechanisms, and properties. These polymers have been seen in applications such as OLEDs, FETs, and rechargeable batteries. Conjugated polymers also seem to have many future applications, some of which include photovoltaic cells, electronic paper, printable circuit boards, and sensors.

Student Technical Division Poster Contest: EPD - Graduate Level

(9) Aluminum Electrowinning and Electrowinning in Ionic Liquid Electrolytes: *Mingming Zhang*¹; *Ramana G. Reddy*¹; ¹University of Alabama

Aluminum electrowinning/electrorefining in ionic liquids were investigated on both laboratory and batch recirculation scales. The cell performance variables studied were the aluminum ion concentration and current efficiency as a function of current density and process time. The results showed the current efficiency of 80%-90% can be achieved at temperature range of 80-120°C. Based on experimental results, a mathematical modeling for predicting current density distribution was developed by assuming steady state, binary electrolyte and constant properties. The model describes the deposition process by incorporating the mass transport of participating ionic species, homogeneous chemical reactions, and the associated electrochemical kinetics. The modeling results showed the computed current densities are in good agreement with experimental data at applied cell voltage less than 3.5 V. Optimum electrode distance was determined to be 1.0-1.5 cm under batch recirculation experimental conditions.

(10) Characterization of Intercalation and Melt-Related Phenomena of [001] Single-Crystal W Ballistic Penetrators Interacting with Steel Targets: *Carlos Pizaña*¹; *Isaac Anchondo*¹; *Aditya Putrevu*¹; *Lawrence E. Murr*¹; *Thomas L. Tamoria*²; *H. C. Chen*²; *Sheldon J. Cytron*²; ¹University of Texas; ²General Atomics

In-target residual [001] single-crystal tungsten penetrators have been characterized by light and electron microscopy in this study. The post-impact (velocities ranging from ~1100m/s to ~1300m/s) residual penetrators examined revealed unambiguous evidence of target (steel) and penetrator (tungsten) intercalation and/or alloying. Considerable mixing activity was found to concentrate specifically within the material being eroded by DRX-assisted flow. The solid-state flow features including shear bands and other flow-induced phenomena seem to facilitate the mixing of the two. Peripherally along the head of the penetrator and usually adjacent to and/or as part of the shear band itself, large bands of Inconel-178 appear to influence the solid-state flow

of the penetrator ultimately affecting the penetration performance. Residual microstructures (dendrites) obtained on some areas within the penetrator suggest localized melt zones due to thermal instabilities caused by the turbulent behavior of flow in the high-pressure regime. Supported by the U.S. Army TACOM-Picatiny Arsenal.

(11) Electrochemical Studies of the Influence of Ore Mineralogy on the Bioleaching of Complex Sulphide Ores: *Peter A. Olubambi*¹; Herman Potgieter¹; Sehiso Ndlovu¹; Joseph O. Borode²; ¹University of the Witwatersrand, Johannesburg; ²Federal University of Technology, Akure, Nigeria

The influence of ore mineralogy on the bioleaching of complex sulphide ore was studied using electrochemical methods. Bioleaching at pH of 1.6 and stirring speed of 150 rpm was initially conducted using mixed cultures on mesophiles with special reference to zinc, copper and iron dissolution. Zinc dissolutions were higher than copper, while the amount of Fe dissolved initially increased but reduced at longer bioleaching days. Potentiodynamic technique was used to study dissolution behaviour for 21 days using massive electrodes prepared from different mineral rich phases of the bulk ore. Characteristics polarization curves showed that sphalerite rich phase had the highest dissolution rate while very complex phase had the least dissolution. The morphologies and structures of bacterial attacked surfaces were examined by the scanning electron microscopy.

Student Technical Division Poster Contest: LMD - Graduate Level

(12) Numerical Modelling of Deformation Phenomena in Magnesium Alloys: *Julie Levesque*¹; Kaan Inal¹; Kenneth W. Neale¹; ¹University of Sherbrooke

In this paper, a new constitutive framework based on a rate-dependent crystal plasticity theory is presented to simulate large strain deformation phenomena in HCP metals. In this new model the principal deformation mechanisms considered are crystallographic slip and deformation twinning. The new framework is incorporated into in-house finite element (FE) codes. Simulations of uniaxial tension and compression for the magnesium alloy AM30 are performed and results are compared with experimental observations at different temperatures. Limitations of the current modelling approaches are also discussed.

(13) Modeling Methods for Managing Raw Material Compositional Uncertainty in Alloy Production: *Gabrielle Gaustad*¹; ¹Massachusetts Institute of Technology

Operational uncertainties create inefficiencies in metal alloy production. One that greatly influences remelter batch optimization is variation in raw material composition, particularly for secondary materials. Currently, to accommodate compositional variation, firms commonly set production targets well inside of the window of compositional specification required for performance reasons. Window narrowing, while effective, does not make use of statistical sampling data, leading to sub-optimal usage of secondary materials. This paper explores the use of a chance constrained optimization method, which allows explicit consideration of statistical information on composition. The framework and a case study of cast and wrought production with available scrap materials are presented. Results show that it is possible to increase scrap consumption without compromising the likelihood of batch errors, when using this method compared to conventional window narrowing.

(14) TiN Coating for Metallic Bipolar Plates of Direct Methanol Fuel Cell (DMFC): *Biswa R. Padhy*¹; Ramana G. Reddy¹; ¹University of Alabama

Direct methanol fuel cell (DMFC) is a promising technology to perform, as a portable energy source for commercial, automobile and military applications. Bipolar plate is an important component of DMFC, which has intricate flow field design machined on it and carries 80-85 % weight of the whole stack. Emphasizing more on issues like weight, fabrication cost and availability, this was concluded that metals/alloys are probable candidate for the bipolar plate and Al-6061 was selected as a material for bipolar plate. Long term stability test was carried out and MEA was characterized by EDS, and XPS. The aluminum from the end plates were leached and 23 % by weight fraction of MEA surface was found as aluminum. To avoid the dissolution of Al-6061 end plates, it was coated with TiN using spray technique and performance of DMFC with TiN coated Al-6061 bipolar plate was investigated.

(15) Nanostructure of High-Temperature Precipitation-Strengthened Al-Sc Alloys with Ternary Additions (Ti, Gd or Yb): *Marsha E. Van Dalen*¹; David C. Dunand¹; David N. Seidman¹; ¹Northwestern University

Ternary additions can improve the properties of dilute Al-Sc alloys that contain nanometer size, coherent Al₃Sc precipitates (L1₂ structure). Ti additions are added to increase the coarsening resistance of the precipitates. Rare earth (RE) elements (Gd or Yb) are found to substitute for Sc forming Al₃(Sc_{1-y}RE_y) precipitates. RE additions lead to an increased number density of the L1₂ precipitates resulting in an increase in hardness by a factor of three over binary Al-Sc alloys. Transmission electron microscopy and atom-probe tomography are utilized to analyze the chemical composition and coarsening kinetics of the precipitates. Segregation at the heterophase interface between α -Al and Al₃(Sc_{1-y}X_y) is examined (X = Ti, Gd or Yb).

Student Technical Division Poster Contest: LMD - Undergraduate Level

(16) Metallurgical and Acoustical Characterization of an Aluminum Alloy (6061) Caribbean Pan: Maria Isabel Lopez¹; Sara M. Gaytan¹; ¹University of Texas

In this study an aluminum pan was produced and compared with a standard steel Caribbean pan. The pan was produced by cold rolling and heat treating 6061-Al. Microhardness testing, transmission electron microscopy and acoustic readings were performed to analyze its effectiveness. Chromatic tones were observed for most rim notes, but the highest octave range notes at the pan bottom were not tuned. Microstructural characterization through optical metallography, hardness testing, and transmission electron microscopy reveal the aluminum pan was not fully tuned since a high dislocation density and related hardness required to stabilize notes to achieve chromatic tuning was not observed.

(17) Characterization of Aluminum Boron Copper Composites for Aerospace Applications: Ruth G.I. Hidalgo¹; Sandra Pedraza¹; ¹University of Puerto Rico

The objective of the work was to analyze and characterize Al-B and Al-B-Cu composites, which have been proposed as alternative material for aerospace applications. These materials were prepared by casting Al 5% B alloys with copper between 0 and 5 wt%, which were rapidly solidified. The purpose was to characterize the distribution of the AlB reinforcing particles embedded in the aluminum matrix without and with the influence of copper, at the microscale. The characterization techniques used included atomic force microscopy (AFM), scanning electron and optical microscopy, and Vickers microhardness. To enhance the topography for AFM imaging, all samples were microetched. The 3-D images allowed identifying AlB particles and grain boundaries as well as Cu-containing phases. Also, the location of the matrix grain boundaries with respect to the diboride was observed. This helped characterize surface topography and determine the size and shape of reinforcements on the composite surface.

(18) The Effect of Manganese Oxide and Iron Oxide Mold Flux Phase of Slag Disc Chemistry in Continuous Casting: Jui-Hung (Harry) Chien¹; Wanlin Wang¹; ¹Carnegie Mellon University

The study of the effect of the different mold flux solidification on radiative heat transfer has not been conducted widely, although it has been used to moderate the heat transfer rate in continuous casting. To simulate the radiative heat transfer phenomena in continuous casting, an infrared radiation emitter was developed to allow heat fluxes of about 1 MW/m² to be applied to a copper mold covered with solid slag disc. The mold flux disc was made by different compositions of either manganese oxide or iron oxide. The response from the in-mold thermocouples indicated that the effect of having a low concentration of manganese oxide or iron oxide mold flux increase the heat transfer rate and then as the thickness of these mold flux increases, the heat transfer rate also increases. This demonstrates a significant potential of using these mold flux to control the heat transfer rate during continuous casting.

Student Technical Division Poster Contest: MPMD - Graduate Level

(19) A Research Study on the Production of Advanced High Strength Steels (ULSAB-VAC), Applied in Auto Structural Parts for the Optimization of Auto Fuel Performance: Shahrokh Pourmostadam¹; ¹Mobarakeh Steel Company

With regard to the achievement of the latest global Technologies for the optimization of energy consumption performance in Autos. It is worth quoting that Auto makers and steel producers of the world have initiated their efforts on the production of advanced high strength steels in low thicknesses with suitable formability. The trial production of AHSS steels focusing on the following objectives: 1) reduce Auto body weight up to 36%, 2) utilize the latest technologies, 3) achieve satisfactory performance of the Auto body during accidents, 4) decrease fuel consumption, 5) prevent environmental pollution. The trial production of AHSS based on B53-3316 standard applied on Peugeot and Citroen cars. In this study, efforts are made to present the chemical analysis and Mechanical properties of the coils produced in the trial running in addition to the characteristics of AHSS in relation to the optimization of strength, the effective thickness reduction of car weight and fuel consumption reduction.

(20) High-Temperature Tensiometry: Ala Moradian¹; Javad Mostaghimi¹; ¹University of Toronto

Modern technology rests on the science of measurement, and the more advanced a technology becomes the more critical are the demands which are placed on the accuracy of measurements. Metal manufacturing and fabrication industries are increasingly using mathematical based models to obtain a better understanding of the processes. These models rely on the accuracy of the physico-chemical properties. Surface tension of high melting point materials was studied by the new experimental/numerical procedure presented. Samples were melted by using a rf-ICP plasma torch. The method was

based on the dynamics of the melting; and the calculations were based on matching the theoretical and numerical dynamics on the experimental observations. The comparisons were performed by the means of image analysis algorithms. In addition to the qualitative agreement in the dynamics of the phenomenon, the quantitative values are close to the expected values repeated from different methods.

(21) Energy Savings in Forging and Heat Treatment of an Aluminum Alloy Subjected to Severe Plastic Deformation: Balakrishna Cherukuri¹; Raghavan Srinivasan¹; Prabir Kanti Chaudhury²; ¹Wright State University; ²Orbital Sciences Corporation

Aluminum alloy AA6061 was SPD (Severe Plastic Deformation) processed by Equal Channel Angular Pressing (ECAP) to study the effect of accumulated strain on the hot workability and heat-treatment response of the alloy. In this study, O and W tempered AA 6061 samples were subjected to severe plastic deformation at room temperature by ECAP (Route BC), producing 50 mm and 100 mm square billets. Hot workability of O tempered material was determined by forging industrial parts at various temperatures. Heat treatment studies were carried out on as pressed W tempered material. Results show that both the forging temperature of the billets and the starting billet size can be substantially decreased compared to conventional forging practice. Peak hardness was obtained at shorter heat treatment times compared to that of the conventional material. Forging at lower temperatures, decreased material usage, and heat treatment at shorter times indicate that significant energy savings are possible.

(22) A Study of Gas Atomized Powder and Melt Spun Ribbon for Improved $MRE_{2/3}Fe_{1/3}B$: Peter K. Sokolowski¹; I. E Anderson²; W. Tang²; Y. Wu²; K. Dennis²; M. Kramer²; R. McCallum²; ¹Iowa State University; ²Ames Laboratory

Rapid solidification of novel mixed rare earth-iron-boron ($MRE_{2/3}Fe_{1/3}B$) alloys via high pressure gas atomization (HPGA) can promote similar magnetic properties and microstructures as closely related alloys produced by melt spinning at low wheel speeds. The primary differences in solidification microstructure are related to distinctions in heat transfer mechanisms and directionality. By producing HPGA powders with the desirable qualities of melt spun ribbon, the need for crushing ribbon is eliminated. The spherical geometry of HPGA powders is more ideal for processing of bonded permanent magnets since higher loading fractions can be utilized during compression and injection molding. An increased volume loading of spherical PM powder can yield a higher maximum energy product (BH_{max}) for magnets to be used in high performance applications. Support from DOE-EERE-FCVT through Ames Lab contract W-7405-ENG-82.

(23) Interfacial Phenomena in Carbon Nanotube Reinforced Aluminum Composite Structure Fabricated by Plasma Spray Forming: Tapas Laha¹; Arvind Agarwal¹; ¹Florida International University

Successful fabrication of free standing Al based nanocomposite structure by plasma spray forming has been demonstrated in this present study, where hypereutectic Al-21wt%Si alloy has been reinforced with multiwalled carbon nanotube. Homogenous distribution of physically intact and undamaged carbon nanotubes has been observed in the plasma spray formed nanocomposite structure. The interfacial aspects and wettability of Al-Si alloy and CNT has been emphasized as interfacial structure dominates the load transfer from the matrix to the higher strength CNT reinforcement. The effect of silicon as alloying element on wettability of aluminum alloy on CNT has been studied with thermodynamic considerations. An ultrathin continuous silicon carbide layer formation on CNT surface suggests increased wettability of molten hypereutectic Al-Si alloy on CNT. TEM investigations validate the formation of very thin product layer (2-5 nm) at the interface of CNT and Al-Si matrix.

(24) Effect of Carrier Gas on Microstructure, Corrosion and Mechanical Properties of Cold Sprayed 1100 Aluminum Coatings: Srinivasa R. Bakshi¹; Kantesh Balan¹; Tapas Laha¹; ¹Florida International University

Two different coatings of 1100 Aluminum were deposited onto similar substrate, using 100 vol.% He and mixture of He-20 vol.% N_2 as carrier gases. TEM investigation revealed a shock wave structure with restrained flow lines and dislocation piling in He processed coating and sub-grain formation in He- N_2 processed coating which is responsible for higher hardness of He processed coating. Elastic modulus of the coating/substrate system was found to be same and equal to that of Al 1100 (69 GPa). The Mode I fracture toughness of the coating/substrate system was found to be more in case of He- N_2 processed coating (6.5 MPa.m^{1/2}) than the He processed coating (4.2 MPa.m^{1/2}). SEM of the delaminated surface shows higher degree of brittle failure of the interface in the He processed coating than the He- N_2 processed coating.

(25) Solidification Microstructures with Solidification Rates and Thermal Gradients in Single Crystal Superalloys, CMSX-4 and CMSX-10: G.S. Choi¹; Jehyun Lee¹; S.H. Kim¹; S.M. Seo²; D.H. Kim²; C.Y. Jo²; ¹Changwon National University; ²Korea Institute of Machinery and Materials

Directional solidifications have been studied at various thermal gradients, 13 ~ 23°C/mm and solidification rates, 1~100 μm/s in CMSX-4 and 10 single crystal superalloys. In this experiment, high thermal gradient could be obtained by applying the liquid metal, such as Ga-In, as a cooling media in directional solidification apparatus, and also by adjusting the cold chamber in the Bridgman system. Higher thermal gradient contributed to reduce dendrite arm spacing effectively, which results in reducing the size of eutectic, as well as higher solidification rate. The primary and secondary dendrite spacings of single crystal superalloy were compared the other superalloys. The length of the mushy zone decreased with increasing thermal gradients and increased with increasing solidification rates. Solidification fraction and segregation were also analyzed between dendrites.

(26) Solidification Microstructure and Phase Transformation Temperature Analysis in the Ni-base Superalloy 738LC: S.S. Gang¹; Jehyun Lee¹; Y.H. Kim¹; J.S. Lee¹; C.Y. Jo²; U. Paik³; ¹Changwon National University; ²Korea Institute of Machinery and Materials; ³Hanyang University

This paper belongs to the materials processing and manufacturing division (MPMD) and graduate student contest. Solidification microstructure and solidification behavior were studied by directional solidification in the In738LC. Directional solidification experiments were carried out at solidification rates of 1-100 μm/s and under thermal gradients of 100-200°C/cm. The solid/liquid interface changed from planar to dendritic, and also the dendrite spacing decreased and dendrite length increased with increasing solidification rate. The carbide morphology also changed from blocky, script, to spotty shape as increasing solidification rate. The phase transformation temperatures, such as, the solidification starting temperature, carbide formation temperature, and eutectic temperature, were estimated by comparing DTA and solid/liquid interface morphology.

(27) Study on The Load-Deflection Characteristics of Diaphragm Springs: Yusuke Sawaguchi¹; ¹Doshisha University

In diaphragm springs manufacturing, setting is applied to improve the endurance limit while setting changes the load-deflection curve of the spring. The purpose of this study is to reveal the reasons why the load-deflection curve changes due to setting. Strains in the tangential direction of the spring and their variation were measured during setting for sample diaphragm springs. The stress distribution in the same direction was calculated by FEM. The following conclusions were obtained. 1. The residual stress in the tangential direction is widely and unequally distributed over the spring after setting. The load-deflection characteristics change due to the residual stress. 2. Anti-plane deformation occurs at the bottom of the levers during setting. Consequently a large compressive stress in the tangential direction occurs. Therefore, the excessive setting improves endurance of the diaphragm spring as well as shot peening.

(28) Improving the High Temperature Wear Characteristics of Industrial Tools, Dies and Processing Equipment Using Functionally Graded Refractory Metals: *Sudip Bhattacharya*¹; Jerrod A. Roalstad¹; ¹South Dakota School of Mines and Technology

The goal of this investigation is to improve the high temperature wear and corrosion characteristics of currently used H13 industrial tool and die surfaces by depositing functionally graded layers of metals in order of increasing melting temperatures. The depositions were done using a 3 kW Nd: YAG laser. The metals considered for deposition are Nickel, Chromium, Molybdenum, Niobium, Vanadium, Tungsten and Tantalum based on the desired properties and extent of solid solubility. Initially the binary pair combinations of Fe(H13)/Cr, Fe(4340 & H13)/Ni, Fe(H13)/V, Cr/Mo, Cr/Nb, Cr/V, Cr/Mo, Nb/Ta, Nb/V, Nb/W, Ni/Cr, Mo/Ta, Mo/W, V/Ta were selected for investigation. Except Fe (4340)/Ni, Cr/Mo and Mo/W other pairs exhibited good bonding. Based on the results of the binary pairs the functionally graded layers of Ni/Cr, Cr/Nb, Nb/Ta (or W) is being investigated. The possible functionally graded set of metals to be considered for deposition are Fe/Cr/ Nb/W (or Ta) or Fe/Cr/V/W (or Ta).

(29) Thermal Stability of Refractory Alloys Deposited on H13 by Laser Powder Deposition: Jerrod A. Roalstad¹; *Sudip Bhattacharya*¹; ¹South Dakota School of Mines and Technology

The goal of this ongoing investigation is to improve the wear characteristics of industrial tools and dies by laser depositing refractory materials like cemented tungsten carbides and super alloys onto their working surfaces. The alloys NiTun60, Co-WC, CCW+, AeroMet, and DM21 were deposited onto H13 surfaces and actual tools and dies using a 3-KW Nd: YAG laser. Samples of these depositions have been tested for thermal stability, wear resistance, and other mechanical properties. Computational softwares, ThermoCalc and DICTRA, were used to model these tests and the progression of phases formed during the tests. The simulated results were then compared with the actual test results. Tools with these laser deposited surfaces were run in an actual production setting. All alloys except DM21 showed a significant improvement over typical H13 tool life.

(30) Evaluation of Optical and Electronic Properties in Nanocrystalline Cerium Oxide Using UV – Vis Spectroscopy: *Satyanarayana Kuchibhatla*¹; Ajay Karakoti¹; Ranjith Tanneru¹; Sudipta Seal¹; ¹University of Central Florida

There has been an increasing interest in using nanocrystalline cerium oxide in optical, electronic and biological applications. The non stoichiometry, mixed valence states, size and morphology are the key factors that control various properties. Current work is an effort to use the UV-VIS spectroscopy and High Resolution Transmission Electron Microscopy to correlate the size dependent physico-chemical properties of nanocrystalline cerium oxide. Transmission spectra obtained as a function of time, concentration and the solvent are used to evaluate the nucleation and agglomeration behavior. Results from the nanocrystalline ceria through wet chemical synthesis using DI water, ethylene glycol and Poly (ethylene glycol) in various concentrations will be discussed. An effort shall be made to explain the variation in the band gap as a function of time, which in turn can lead to an understanding of nucleation, growth and agglomeration kinetics.

Student Technical Division Poster Contest: MPMD - Undergraduate Level

(31) Teaching Modules Development at Rensselaer Polytechnic Institute: *Afina Lupulescu*¹; Martin Eden Glicksman¹; Elvin Eng¹; ¹Rensselaer Polytechnic Institute

By selectively integrating our research interests and teaching methods we developed a series of lecture modules covering the basics of 1) solid-state diffusion, 2) kinetics of materials processes, 3) solidification and crystal growth. These include 24 teaching modules based on the textbook, Diffusion in Solids: Field Theory, Solid-State Principles and Applications¹, and 26 lecture modules supporting a first course in undergraduate kinetics of materials processes, which are coordinated with the textbook, Physical Foundations of Materials Science². An additional 25 modules are scheduled for release in Spring 2006, which focus on advanced topics in solidification, melting, and crystal growth. The authors are grateful for support provided under grant NSF-DMR 0303813. ¹M.E. Glicksman, Diffusion in Solids: Field Theory, Solid-State Principles and Applications, John Wiley & Sons, New York (2000). ²G. Gottstein, Physical Foundations of Materials Science, Springer, Berlin (2004).

(32) Preparation of LAST Thermoelectric Powders by Planetary Ball Milling: *Adam L. Pilchak*¹; Fei Ren¹; Eldon D. Case¹; ¹Michigan State University

Thermoelectric materials are often cast as ingots, however, the ingots often have large grain sizes and consequently low mechanical strength. Crushing and milling the cast ingots can produce fine powders which can be sintered to prepare thermoelectric materials with fine grain sizes. Small grain sizes not only improve mechanical strength, but can also lower thermal conductivity by increasing phonon scattering mechanisms at grain boundaries. A reduction in thermal conductivity can increase the thermoelectric figure of merit, ZT. In this study, Lead-Antimony-Silver-Tellurium (LAST) powders are prepared by planetary ball milling. The effect of milling time and grinding media on the particle size distributions is presented. Furthermore, a pre-milling treatment is used to increase the efficiency of the planetary mill.

(33) Determination of the Optimum Temperature and Strain for Open-Die Forgings of Ti-6Al-4V ELI at Beta-Phase Temperatures: *Robert J. Weiss*¹; ¹The Boeing Company

Forging of titanium in the beta-phase region has the potential to reduce the process complexity of alpha-beta forged titanium by offering fewer steps and closer net-shape configurations. This study attempts to optimize the temperature (1000°C - 1300°C) and total strain (25% - 75%) processing window for Ti-6Al-4V ELI beta-forgings. Vickers microhardness and microstructures were collected along with data for strain rate, transfer time, and press load to characterize the process. Response surface and prediction techniques quantified variation in hardness according to the process combinations, revealing an increasing trend in strength for increases in both temperature and strain. The model shows consistency in hardness near the beta-transus for all the levels of strain studied. One inaccuracy encountered was the inability of small forgings to model large scale material deformations; most notably, large amounts of Widmanstatten structure, possibly ascribed to greater cooling rates than those found in current titanium processes.

(34) Microstructure Effects on Tin Whisker Growth : Jonathan P. Winterstein¹; M. Grant Norton¹; ¹Washington State University

Tin whiskers present a significant reliability issue for tin-plated microelectronics. Tin whisker growth on electroplated films on 99.9% pure copper substrates was studied using SEM. Films approximately 1 μm thick were plated at different current densities and temperatures. The effects on whisker growth of electroplating process parameters and post-deposition heat treatments were related to microstructural features of the films. Results indicate film porosity may limit whisker growth. Samples plated at lower current density showed less porosity and whiskers were observed 12 days after deposition while samples plated at higher current density were more porous and some samples plated at higher current density showed no whisker growth 33 days after deposition. Also, initial whisker growth rates of approximately 0.082 nm/s were determined. Understanding microstructural effects on whisker growth will provide insight into possible nucleation and growth mechanisms and may lead to approaches to prevent whisker formation.

(35) Evaluation of Nanocrystalline Powder Assisted Spot Welding of Aluminum : Diana Chan¹; Selina Brownridge¹; Yuranan Hanlumyung¹; Jui-Hung Chien¹; ¹Carnegie Mellon University

The use of nanocrystalline aluminum powders to improve the spot weldability of smooth and mechanically surface textured aluminum sheets is evaluated. These nanocrystalline powders are capable of releasing energy well below the melting temperature of aluminum and therefore could be capable of reducing the energy required in spot welding aluminum. Textured aluminum sheets were chosen to entrap these powders during forming and welding. Powders were applied to both textured and smooth aluminum sheets, which were then spot welded at different currents to evaluate weldability. Smooth aluminum sheets without powders served as the control. Measurements of lap shear strength and weld nugget diameter indicated that the powders assisted in producing acceptable welds at lower currents than those needed to produce acceptable welds in the same sheets without powders. This demonstrates significant potential for using these powders to reduce the energy required to spot weld aluminum.

(36) The Feasibility of High Grade X100 Steels in Northern Gas Pipelines : Jennifer Cutting¹; ¹The University of British Columbia

There is an increased need for oil and gas production from northern Canada and Alaska. The possibility of constructing northern gas pipelines from X80, X90, and X100 steel was investigated. Using higher grade steels decreases overall construction costs and material volume and increases gas transfer rates. The design, performance, and production feasibility of high grade pipeline steel was examined. Possible hot rolling schedules were proposed using a computer simulation and a run-out table model was constructed to determine required cooling rates. Thermomechanical rolling and cooling lab simulations were performed. Relevant properties of the steel test specimen were recorded. Weld simulations and tests were also done. Up to X100 grade steel appeared technically suitable in terms of performance. The examined north american steel manufacturing facilities did not appear to be currently capable of achieving the cooling rates suggested by this study.

Student Technical Division Poster Contest: SMD - Graduate Level

(37) The Effects of Hf Addition on the Glass-Forming Ability and Mechanical Properties of Cu-Based Bulk-Metallic Glasses : Dongchun Qiao¹; Peter Liaw¹; ¹University of Tennessee

The glass-forming ability and mechanical properties have been investigated in Cu_{47.5}Zr_{47.5-x}Hf_xAl₅ (x = 0, 9.5, 19, 28.5, 38, and 47.5). The glass-transition temperature (T_g), crystallization temperature (T_x), melting temperature (T_m), and liquidus temperature (T_l) were measured by the differential-scanning calorimetry (DSC) and differential-thermal analyzer (DTA). The structure was detected by X-ray diffraction (XRD). CuZr precipitated with the increasing of Hf content from 9.5 % to 28.5 % and disappeared when Hf content reached to 38%. The materials under compression tests show some plasticity due to the precipitation of the CuZr phase, compared with the BMG without the Hf addition.

(38) Corrosion-Fatigue Study of Hastelloy® C-2000®: Structural Materials Division, Graduate Student Submission : Rejanah V. Steward¹; Raymond A. Buchanan¹; Peter K. Liaw¹; ¹University of Tennessee

Hastelloy® C-2000® Alloy is a commercially designed superalloy manufactured to function in both reducing and oxidizing solutions. Its industrial applications have tremendous potentials in automotive, structural, aviation, and storage components. The objective of this study is to thoroughly examine the fracture morphology of C-2000® and understand the damage evolution from the incipient crack-initiation to final fracture after the subjection to mechanical stresses in air and 3.5 weight percent (wt. %) NaCl. Experimental measured parameters will be used in a lifetime-prediction model to simulate failure. Electrochemical tests were employed to determine electrochemical parameters, and electron microscopy and in-situ macro-visualization were used to observe and monitor crack initiation and propagation behavior of C-2000®. Crack initiation originated from the subsurface within the grain structure and traversed the grains to the final fracture. The life spent in crack initiation was drastically reduced under maximum stress conditions and decreasing frequencies in 3.5 wt. % NaCl.

(39) Severe Plastic Deformation Induced Fe-W Alloy Composite Formation by Mechanical Mixing of Fe and W : Aditya Putrevu¹; C. Pizaña¹; Lawrence E. Murr¹; I. A. Anchondo¹; T. L. Tamoria²; H. C. Chen²; S. J. Cytron³; ¹University of Texas; ²General Atomics; ³U.S. Army TACOM-ARDEC

Optical metallography and SEM in combination with microhardness maps have been used to elucidate the dynamic recrystallization (DRX)-facilitated flow and interaction of steel targets with penetrating, un-clad [001] single-crystal W long rods impacting at initial velocity of 1.3 km/s. The ultra-fine DRX regime composing adiabatic shear zones in both the penetrator and target allows for mechanical mixing of the W and Fe in complex flow regimes which, in the extreme, melt in localized regions at the projectile/target interface. The Fe-W interface, characteristic of complex flow regimes, revealed a varying character. There was evidence of both localized melting and formation of an Fe-W solid solution, and associated dendritic nucleation and growth and mechanical mixing of Fe and W to form a composite region, in this high-strain-rate, high-pressure regime. Supported by the U.S. Army TACOM-Picatiny, Prime Contract No. W15QKN-04-M-0267, project No. 1A4CFJER1ANG.

(40) Kinetics of Secondary γ in Ni-base PM Superalloys: Heather Sharpe¹; ¹Georgia Institute of Technology, Rolls-Royce

To increase engine efficiency, gas turbine disks must withstand an increasingly demanding operating environment. More advanced alloys and increased microstructural control are the key to producing Ni-base powder metallurgy disks capable of higher temperature operation. This study focused on the microstructural aspects of the development of these disk alloys, specifically the control of grain size and secondary γ morphology. Three representative PM Ni-base alloys, LSHR, RR1000, and Alloy 10, have been subjected to a series of controlled cooling rates to establish the kinetics of secondary γ formation. Quantification of morphological characteristics such as precipitate size, orientation, and concavity was done by computational image analysis.

(41) The Physical Properties of Nylon-66/Ferrite Nano Hybrids: Sang Jin Lee¹; Dong Wook Chae¹; Ki Hyun Lee¹; Byoung Chul Kim¹; ¹Hanyang University

Ferrite nanoparticles (0.1–20 wt%) were incorporated into the nylon-66 by melt-compounding and their effect on the physical properties were investigated. The presence of ferrite nanoparticle less than 1 wt% increased the crystallization temperature (T_c) by 4.2 °C with the loading level, but after the value it decreased T_c with the loading level. The incorporation of ferrite nanoparticle up to 1 wt% had little effect on the dynamic viscosity (η') but after the value it increased the η' with the loading level. In particular, the nanohybrids with ferrite more than 5 wt% exhibited notably shearing thickening behavior in the low frequency and then shear thinning was followed showing that its degree increased with the loading level. The tensile strength increased a little with the loading level of ferrite up to 1 wt% but after the value it decreased with increasing the loading level.

(42) Effects of Silver Nanoparticle on Rheological and Other Physical Properties of Syndiotactic Polypropylene: Seung Han Park¹; Dong Wook Chae¹; Byoung Chul Kim¹; ¹Division of Applied Chemical Engineering

The Syndiotactic-polypropylene (sPP)/silver nanocomposites were prepared by melt compounding. The effects of introducing silver nanoparticle on the rheological and other physical properties of syndiotactic PP were investigated. The silver nanoparticles were well dispersed in the sPP matrix. sPP containing 5 wt% silver nanoparticle presented higher crystallization temperature (T_c) and heat of crystallization (ΔH_c) than pure sPP by 12.3 °C and 4.1 J/g, respectively. DSC melting endotherms exhibited double melting phenomena in the vicinity of 121 and 129 °C when crystallized at 90 °C under shear. On the contrary, the samples crystallized at 100 °C under shear gave a single melting peak at about 126 °C. The modulus of the sPP composites increased a little with increasing the loading level of silver nanoparticle. Elongation to break increased up to loading level of 0.1 wt%, after which it decreased with increasing the loading level.

(43) Physical Properties ZnO Nanoparticle-Filled Polyacrylonitrile: In Kyu Song¹; Dong Wook Chae¹; Byoung Chul Kim¹; ¹Division of Applied Chemical Engineering

PAN/ZnO nanocomposites were prepared by a solution mixing in dimethylacetamide (DMAc) as a co-solvent and then film casting. PAN solutions with ZnO nanoparticles showed higher dynamic viscosity (η') than the pure PAN solution. They showed maximum at the loading level of ZnO, 1 wt%. PAN solutions with 5 wt% ZnO showed greater degree of shear thinning than the others. The Cole-Cole plot of PAN solutions didn't give a master curve independent of ZnO concentration. TEM revealed that ZnO nanoparticles were homogeneously dispersed within the PAN matrix. The heating scan of DSC displayed only a single crystallization peak (T_c) without melting peak regardless of the presence of ZnO. The introduction of ZnO nanoparticles decreased T_c by ca. 13 °C, and increased the heat of crystallization by ca. 18% in comparison with pure PAN. Further, the nanoparticle improved the thermal stability of PAN greatly.

(44) Adiabatic Shear Bands Associated with Plug Formation and Penetration in Ti-6Al-4V Targets: Formation, Structure, and Performance: Fabiola Martinez¹; Erika V. Esquivel¹; Maribel I. Lopez¹; Sara M. Gaytan¹; Diana A. Ramirez¹; David A. Lopez¹; Amanda Ramirez¹; Pricilla A. Guerrero¹; Carlos Pizana¹; Isaac Anchondo¹; Larry E. Murr¹; B. E. Schuster²; M. Fermen-Coker²; ¹University of Texas; ²U.S. Army Research Laboratory

A series of electron beam, cold hearth, single melt Ti-6Al-4V plates (nominally 2.5 cm thick) impacted by 2cm diameter, 4340 steel projectiles (with 54g nominal mass) at velocities ranging from 0.633 to 1.027 km/s were sectioned along the impact axis and examined by optical metallography, SEM, and TEM to characterize the formation, growth, and microstructure of adiabatic shear bands which facilitate plug formation and projectile perforation by dynamic recrystallization (DRX) within the shear bands; allowing for solid-state flow. The localized DRX of the projectile and projectile-target interaction phenomena were also examined using elemental X-ray mapping of the targets and projectiles in the SEM. Near ballistic limit velocities, the shear bands propagate towards the rear of the target where they coalesce and grow to provide a cylindrical (DRX) flow regime for the plug volume (Supported by ARL Prime Contract DATMo5-02-C-0046, Amendment 16).

(45) Effects of Zinc Oxide Nanoparticle on Physical Properties of Poly Styrene: Ki Hyun Lee¹; Dong Wook Chae¹; Byoung Chul Kim¹; ¹Hanyang University

The effects of ZnO nanoparticle on the physical properties of PS were investigated. TEM and FESEM showed that ZnO nanoparticle was homogeneously dispersed in the PS. The introduction of 5wt% ZnO increased slightly the glass transition temperature by 2.38. TGA thermograms showed that the thermal stability of PS was enhanced with increasing ZnO content. Neither shift nor sharpening of absorption band was detected by IR. ZnO had little effect on the wide-angle X-ray diffraction pattern of PS. The transmittance of ultraviolet light was decreased with increasing ZnO content. PS/ZnO nanohybrids exhibited a small reduction in tensile strength and elongation to break. A significant enhancement in tensile modulus was achieved when 5wt% of ZnO was introduced. In the FESEM images of the tensile fractured surface, localized plastic deformation was observed for PS, while the site from which ZnO was pulled out was usually observed in the nanocomposite.

(46) The Rheological and Thermal Properties of PVA/DEG Nanocomposite: Seung Han Park¹; Myung Hwan Chang¹; Byoung Chul Kim¹; ¹Division of Applied Chemical Engineering

The effects of dimethylene glycol (DEG) on the poly vinylalcohol (PVA) solutions in dimethyl sulfoxide (DMSO) were investigated in terms of rheological, thermal and other physical properties. DEG imparted lubricating effects to PVA, increasing flexibility due to ether structure. The dynamic viscosity (η') was decreased with increasing DEG content. The 12 wt% PVA/DEG solutions showed a linear viscoelastic response. The PVA solutions exhibited relaxation time independent of DEG content, when DEG content did not exceed 20 wt%. Above 20 wt% of DEG content, the λ of 6 wt% PVA solutions was decreased in the high frequency range, at high frequency. In addition, the η' of all the solutions was increased with time. The thermal properties of the PVA films containing DEG showed that the crystallization temperature, melting temperature and glass transition temperature (T_g) shifted to lower temperature with increasing DEG content.

(47) Rheological and Other Physical Properties of PVA/PG Solution: *In Kyu Song*¹; Yong Han Cho¹; Byoung Chul Kim¹; ¹Division of Applied Chemical Engineering

The rheological responses of 6 and 12 wt% PVA solutions in DMSO were investigated at four loading levels of a plasticizer, propylene glycol (10, 20, 30, 40 wt% to PVA). The dynamic viscosity of the PVA/PG solutions is generally decreased with increasing PG content. The 12 wt% PVA solution exhibited an abrupt drop of viscosity at 40 wt% PG. On the other hand, the 6 wt% PVA solution showed the abrupt decrease of viscosity from 30 wt% PG. Loss tangent of 12 wt% PVA solutions in DMSO are always less than 1 over the entire frequency range examined irrespective of PG content. 6 wt% PVA solutions containing PG more than 30 wt%, however, showed a phase transition above a critical frequency. The thermal properties of the PG/PVA films suggested that the peak on the $\tan \delta$ curve was decreased with increasing PG content.

(48) Crystallization and Amorphization Behavior of Al90Sm10 Alloy Solidified Far from Equilibrium: *Eren Yunus Kalay*¹; Scott L. Chumbley¹; Iver E. Anderson¹; ¹Ames Laboratory/Iowa State University

The alloy Al90Sm10, a marginal glass former, was rapidly solidified using high pressure gas atomization and melt spinning processes. The resultant gas atomized microstructures were examined as a function of undercooling. Gas atomized particles having different sizes solidify at different cooling rates, thereby providing a large spectrum of undercooling conditions and subsequent solidification microstructures to be explored. The rapidly solidified ribbons are composed of fully amorphous phase. XRD and TEM studies have shown that three different metastable phases accompanied a glassy phase during vitrification. The metastable phases are Al solid solution, tetragonal and orthorhombic Al4Sm. TEM studies of highly undercooled powders showed nanometer sized (15nm) α -Al within an amorphous matrix. Subsequent devitrification behavior of the melt spun ribbons was examined by high temperature time-resolved synchrotron radiation, DSC and TEM. DSC showed three crystallization reactions during devitrification. The product phases of these reactions were identified in situ using time-resolved X-ray diffraction.

(49) Nanocrystalline Metal Indentation: Novel Insights from Atomic Contact Simulation: *Virginie Dupont*¹; Frederic Sansoz¹; ¹The University of Vermont

The plastic behavior of nanocrystalline metal films is strongly correlated to the grain size in nanoscale contact. Despite common knowledge that grain refinement improves strength, high contact stresses have also been shown to cause rapid growth of nano-sized grains. In this poster, atomistic simulations are presented to shed light on the complex relation between grain size and atomic contact in metallic thin films. Specifically, the quasicontinuum theory was used to investigate the cylindrical indentation of single crystal and 5nm-grain size films in Al. The JKR contact model was also adapted to provide insights into the adhesion and mechanical properties of thin films. The major findings of this investigation are that nanocrystalline GB networks strongly impact on the incipient film plasticity; the deformation modes are predominantly GB movement and shear banding mediated by interface sliding; and a relation exists between GB structure, grain growth and evolution of shear stress gradients.

(50) The Design of a Biomimetic Self-Healing Alloy Composite: *Michele V. Manuel*¹; Gregory B. Olson¹; ¹Northwestern University

The principal objective of this research is to use computational design methods to design a self-healing alloy composite that can repair itself in response to structural damage. The self-healing composite is composed of a controlled-melting magnesium-based alloy matrix which is designed for high specific strength and low healing temperatures. The matrix is reinforced by shape memory alloy (SMA) wires that provide crack-bridge toughening during cracking of the composite. When the composite is heated above the reversion temperature of the embedded SMA wires, a clamping force is applied by the SMA wires to provide crack clamping and crack closure at a healing temperature where the matrix alloy is partially molten to provide crack re-welding. Feasibility testing of Sn-Bi prototype composites have displayed a 95% strength recovery. Current testing on magnesium-based composites demonstrates crack closure and an increase in toughness over the unreinforced alloy.

(51) Elastic-Plastic Shock Wave Profiles in Oriented Single Crystals of Cyclotrimethylene Trinitramine (RDX); LA-UR-05-9437: *Kyle Ramos*¹; ¹Washington State University

The molecular crystal cyclotrimethylene trinitramine (RDX) is the main energetic component of many munitions. The mechanical anisotropy of plasticity of RDX has been suggested to control detonation in this material. Plate impact experiments were performed on oriented single crystals of RDX on the (111), (210), and (100) planes to access 3, 2, and 0 slip systems, respectively. Velocity history profiles were measured by Doppler interferometry and utilized to determine the anisotropic dynamic yield point for RDX crystal and provide data for continuum modeling efforts. The resulting data from these experiments show little plasticity differences between the (210) and (100) faces, but show little resistance to plasticity on the (111) face. Complementary experiments with other organic single crystals, which are similar in structure to RDX, using indentation are also presented to demonstrate the ability to resolve dislocation nucleation and multiplication events.

(52) Gas Barrier Properties of Polymer Nanocomposite: *Laxmi K. Sahu*¹; Nandika Anne D'Souza¹; ¹University of North Texas

Polymer nanocomposites based on dispersion of surfactant treated expandable smectite clays such as montmorillonite layered silicates (MLS) have shown promise as organic-inorganic hybrids with the potential to improve barrier properties. Separately, flexible displays based on plastic substrates have reduced lifetimes tied to the low barrier properties. While there has been a general attribution of improved barrier properties to the tortuous path, this does not consider the influence of the introduction of secondary filler on the morphology of the host polymer. In this paper we have taken two semi crystalline polymers, nylon 6 and polyethylene terephthalate (PET) and introduced MLS into the polymers to form nanocomposites. Permeability is predicted taking into consideration the amorphous phase, crystalline phase and MLS content and compared with the experimental values.

(53) Effect of Layered Double Hydroxide (LDH) on Flame Retardant Properties in Poly Vinyl Chloride: *Laxmi K. Sahu*¹; Nandika Anne D'Souza¹; ¹University of North Texas

The thermal degradation of different types of layered double hydroxide (LDH) was studied by Thermo Gravimetric Analysis (TGA). Most common type of LDH is based on a magnesium aluminum hydroxide layer which is used as the base material. This LDH incorporated with nickel metal which leads to partial replacement of magnesium by cationic exchange method which is proved to be the better material. The flame retardant and mechanical properties of the resultant PVC-LDH composites are studied for the flame retardant polymer material applications.

(54) Heat Treatment of the Thermal Spray Objects: Yu-Chih Huang¹; Sinn-Wen Chen¹; *Shih-kang Albert Lin*¹; Chia-Hua Chang²; Jen-Chin Wu²; ¹National Tsing Hua University; ²Chung-Shan Institute of Science and Technology

Spray coating is a unique engineering coating technology. Molten materials spray on substrates to improve surface properties of various substrates. For instance, carbon steels are coated with Al, Ti, and Zn for better corrosion protection. Sprayed objects sometimes are heat-treated to improve the adhesion properties between the coated layer and substrate. Interfacial reactions of sprayed objects during heat treatment are examined in this study. The specimens include TS sample, Zn/steel, and diffusion couples, Zn/Fe-42wt%Ni and Sn-Zn/Fe-42wt%Ni. Alloy42 (Fe-42wt%Ni) is commonly used in the electronic industry. Sn-Zn alloys are promising lead-free solders. Knowledge of interfacial reactions of Sn-Zn/Fe-42wt%Ni is valuable for both

thermal spray of Fe and Ni, and Sn-Zn soldering applications. Because the coating time is very short, for Zn/steel, very thin or no noticeable reaction layers are observed in the as-coated samples. With prolonged heat treatment, δ -phase is found. Γ -phase and Γ' -phase are formed

Student Technical Division Poster Contest: SMD - Undergraduate Level

(55) Investigation of the Effect of Filler Metal on the Microstructure and Microhardness of Inconel 600: *Germanique M. Pickens¹; Viola L. Acoff¹*; ¹University of Alabama

Inconel 600 is a nickel-based superalloy that has excellent corrosion and oxidation properties, especially at high temperatures and also maintains its mechanical strength at elevated temperatures. Inconel 600 is often used to make pressure vessels, aircraft engine parts, and chemical processing components. In this study, Inconel 600 was subjected to gas tungsten arc welding both with and without (autogeneous) the use of filler metal. There was a distinct difference in microstructures observed and the microhardness of the fusion zone for the autogenous welded sample was slightly lower than that was observed for the sampled welded using a filler metal. The purpose of this study is to characterize the microstructure and microhardness of Inconel 600 welded with and without the use of the filler metal.

(56) 3D Microscopy via Serial Sectioning of Shocked Tantalum: Thomas W. Slankard¹; *Daniel Worthington¹*; ¹Los Alamos National Laboratory

Materials characterization has traditionally relied on two-dimensional (2D) representations of inherently three-dimensional (3D) information. 3D information can be subsequently inferred from stereological principles. While this may be sufficient in many cases, some materials require a complete experimentally measured 3D data set to fully capture the true structure. In this work, the 3D microstructure of a shocked tantalum disk was obtained via serial sectioning. Eighty sections of optical micrographs were captured at an average thickness interval of 2.4 microns. Subsequent computer reconstruction of the sections allowed insight into the void morphology resulting from incipient spallation. In addition, spatially specific orientation data was collected every 5 sections using electron backscatter diffraction techniques. Future work will explore the void morphology of samples shocked under different conditions and determine any preferential damage nucleation sites with respect to the grain structure.

TMS Technical Divisions

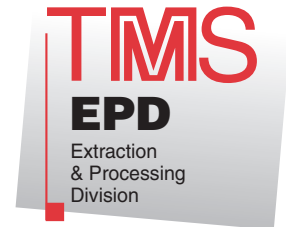


The **Electronic, Magnetic & Photonic Materials Division (EMPMD)** promotes technical exchange and assists in the professional development of its members through programming, publications and continuing education. It addresses the synthesis and processing, structure, properties and performance of electronic, photonic, magnetic and superconducting materials as well as the materials used in packaging, and interconnecting such materials in device structures.

Patrice E.A. Turchi, *Chairperson*

E-mail: turchi1@llnl.gov

The main purpose of the **Extraction & Processing Division (EPD)** is to provide a national and international forum for information dissemination and interaction between industry operators, academics, consultants and managers engaged in the extraction and processing of minerals, metals and materials. EPD addresses three major issues: the emergence of materials; the increasing role of the computer in all facets of processing; and the need to unify the processing field to encompass physical processes, such as solidification and thermomechanical treatment, as well as mineral preparation, extraction and refining. This effort is designed to remove the artificial barriers between extraction, refining and physical processing.



Robert L. Stephens, *Chairperson*

E-mail: rob.stephens@teckcominco.com



The **Light Metals Division (LMD)** is organized to serve professionals in both the traditional (aluminum, magnesium, beryllium, titanium, lithium, and other reactive metals) and emerging (composites, laminates, etc.) light metals fields. This service encompasses recycling technologies and activities related to the materials mentioned. This is accomplished by involvement of academic, research, technical and operational activities toward practical applications of technology.

Ray D. Peterson, *Chairperson*

E-mail: ray.peterson@alcris.com

In its broadest scope, the **Materials Processing & Manufacturing Division (MPMD)** covers manufacturing from product design to production, integrating process control technology into manufacturing (e.g., applying concepts from the intelligent processing of materials to intelligent design and manufacture), and basic and applied research into key materials technologies that impact manufacturing processes (e.g., solidification, powder metallurgy, and shaping and forming). The modeling, simulation and control of materials as they affect manufacturing processes is also a key focus of the division.



John E. Smugeresky, *Chairperson*

E-mail: smug@sandia.gov



The **Structural Materials Division (SMD)** has been chartered to cover the varied aspects associated with the science and engineering of load-bearing materials, including studies into the nature of a material's physical properties based upon its microstructure and operating environment.

Elizabeth A. Holm, *Chairperson*

E-mail: eaholm@sandia.gov

**To learn more about TMS,
its technical divisions or student programs,
visit www.tms.org.**